


# Neptunium(VI) solubility in alkaline $\text{CaCl}_2$ solutions: evidence for the formation of calcium neptunates $\text{Ca}_x\text{NpO}_{3+x}(\text{s,hyd})$

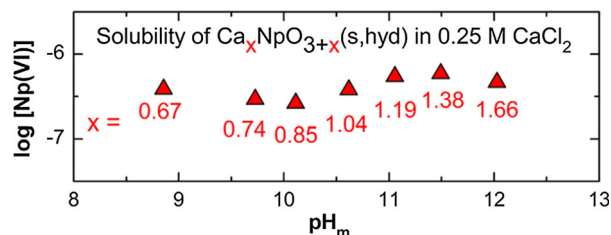
David Fellhauer<sup>1,2,3</sup>  · Xavier Gaona<sup>1</sup> · Jörg Rothe<sup>1</sup> · Marcus Altmaier<sup>1</sup> · Thomas Fanghänel<sup>2,3</sup>

Received: 28 June 2017 / Accepted: 26 November 2017 / Published online: 6 December 2017  
© Springer-Verlag GmbH Austria, part of Springer Nature 2017

**Abstract** The solubility behavior of hexavalent neptunium (Np) was systematically investigated as function of  $[\text{CaCl}_2] = 0.25\text{--}4.5 \text{ mol dm}^{-3}$   $[0.252\text{--}5.26 \text{ mol (kg H}_2\text{O)}^{-1}]$  and  $\text{pH}_m$  8–12 ( $\text{pH}_m = -\log\{m(\text{H}^+)/\text{mol (kg H}_2\text{O)}^{-1}\}$ ) under oxidizing conditions adjusted by hypochlorite. As solubility limiting Np(VI) solid phase, hitherto unknown, non-stoichiometric calcium neptunates,  $\text{Ca}_x\text{NpO}_{3+x}(\text{s,hyd})$ , were identified by applying a wide range of analytical techniques including quantitative chemical analysis, powder XRD, Np L3-edge XANES, and SEM–EDX. The Ca:Np ratio in the equilibrium solid phase increased systematically with the  $\text{pH}_m$  values in the batch solubility samples, and ranged between 0.60:1 and 1.66:1. For  $\text{pH}_m > 10.5$ , the solubility of the calcium neptunates is around  $\log\{[\text{Np}]/\text{mol (kg H}_2\text{O)}^{-1}\} \approx -6.1 \pm 0.4$  and does not show a strong dependence on  $[\text{CaCl}_2]$ . For  $\text{pH}_m < 10.5$ ,  $\log [\text{Np}]$  ranges from  $-6.6$  in  $0.25 \text{ mol dm}^{-3} \text{ CaCl}_2$  to  $-3.6$  in  $4.5 \text{ mol dm}^{-3} \text{ CaCl}_2$ , and increases systematically with  $[\text{CaCl}_2]$ . Based on the solubility data, the principle solid–liquid equilibrium reactions were qualitatively evaluated. The results for Np(VI) obtained in the present work were found to be different from the

behavior of U(VI) in alkaline  $\text{CaCl}_2$  solutions, where the well-defined crystalline  $\text{CaU}_2\text{O}_7 \cdot 3\text{H}_2\text{O}(\text{cr})$  phase controls the U(VI) solubility over a wide range of  $\text{pH}_m$  and  $[\text{CaCl}_2]$  conditions.

*Graphical abstract*



**Keywords** Neptunium(VI) · Calcium neptunates · Hydrolytic behavior · Calcium chloride brines · Thermodynamics · Np L3-edge XANES

## Introduction

Neptunium is a transuranic 5f element (actinide element, An) artificially produced in nuclear reactors and thus present in the spent fuel of nuclear power plants. The main isotope in this context is the long-lived  $^{237}\text{Np}$  ( $T = 2.14 \times 10^6 \text{ a}$ ). Understanding of the aqueous chemistry of An on a sound scientific basis is of high relevance for the long-term safety assessment of underground repositories for nuclear waste disposal with respect to a potential water intrusion scenario, and requires correct chemical and thermodynamic models for the description of the principal geochemical processes of radionuclides in aqueous solution, e.g., the solubility behavior,

**Electronic supplementary material** The online version of this article (<https://doi.org/10.1007/s00706-017-2116-4>) contains supplementary material, which is available to authorized users.

✉ David Fellhauer  
david.fellhauer@kit.edu

<sup>1</sup> Institute for Nuclear Waste Disposal, Karlsruhe Institute of Technology, Karlsruhe, Germany

<sup>2</sup> Institute for Transuranium Elements, European Commission, Karlsruhe, Germany

<sup>3</sup> Institute of Physical Chemistry, Heidelberg University, Heidelberg, Germany

complexation, redox reactions, sorption to mineral surfaces, etc. Like most of the early actinide elements, Np is redox active and can exist as +III to +VI within the thermodynamic border of water stability [1, 2] [note, that Np(VII) is thermodynamically unstable in aqueous solutions, but can form and remain metastable in strongly basic aqueous media with  $[\text{OH}^-]$  typically greater than  $0.5 \text{ mol dm}^{-3}$  in the presence of strong oxidants like ozone  $\text{O}_3$ , or peroxydisulfate  $\text{S}_2\text{O}_8^{2-}$ ]. While Np(III) is only stable in strongly reducing media below  $\text{pH} \approx 3$ , Np(IV) is the predominant oxidation state in reducing environments from slightly acidic to hyperalkaline pH conditions owing to its very pronounced hydrolysis behavior. Np(V) is the most stable actinide in the +V state and prevails especially in “redox-neutral” ( $\text{pe} + \text{pH} = 13.8$  [3]) to oxidizing conditions. Only for hyperalkaline pH values and oxidizing  $E_h$  conditions above the redox-neutral line, Np(VI) becomes thermodynamically stable within the borders of water stability, c.f. [4].

From the last statement it becomes evident that Np(VI) is of less relevance in anoxic, reducing redox milieus which are expected in potential underground repositories. Still, the aquatic chemistry of Np(VI) in especially alkaline solutions remains an interesting and scarcely examined topic from the viewpoint of fundamental actinide research. Only few systematic studies deal with the hydrolytic behavior and the corresponding thermodynamic description of Np(VI) in aqueous solutions and in absence of other complexing ligands. The aquo ion of Np(VI) exists as penta-aqua trans-dioxo-neptunyl complex in acidic solutions,  $\text{NpO}_2(\text{H}_2\text{O})_5^{2+} = \text{NpO}_2^{2+}$ , with the five water ligands perpendicularly bonded to the neptunyl unit (in the equatorial plane) [1, 2]. In most complexed species like the hydrolysis species as well as in many solid phase compounds of An(VI) [and likewise of An(V)], the dioxo structures are retained. The latest NEA–TDB report on Np from 2003 recommends equilibrium constants and parameters for only three aqueous hydroxo complexes,  $\text{NpO}_2\text{OH}^+$  ( $\text{NpO}_2$ ) $_2(\text{OH})_2^{2+}$ , and  $(\text{NpO}_2)_3(\text{OH})_5^+$  from the study of Cassol et al. performed in  $1 \text{ mol dm}^{-3}$   $\text{NaClO}_4$  solutions, and for the binary solid phase  $\text{NpO}_3 \cdot \text{H}_2\text{O}(\text{cr})$  reported by Kato et al. [1, 5, 6]. All species and compounds were studied below  $\text{pH} 7$ . The apparent incompleteness of the chemical and thermodynamic hydrolysis model for Np(VI) is especially striking in view of the well-investigated and expectedly highly analogous U(VI) neighbor element where a large number of monomeric  $[\text{UO}_2(\text{OH})_n]^{2-n}$  with  $n = 1\text{--}4$  and oligomeric hydrolysis species as well as several binary and ternary oxy(hydroxide) solid phases are reported [1].

Recently, Gaona et al. investigated the behavior of Np(VI) in neutral to hyperalkaline TMAOH and NaCl solutions [4, 7]. It was demonstrated that the Np(VI)

solubility is controlled by  $\text{NpO}_2(\text{OH})_2 \cdot \text{H}_2\text{O}(\text{cr})$  in near-neutral pH conditions (for the latter, the same solubility product is considered as for the hydrated trioxide  $\text{NpO}_3 \cdot \text{H}_2\text{O}(\text{cr})$  reported in [1]) and  $\text{Na}_2\text{Np}_2\text{O}_7(\text{cr})$  in more alkaline solutions (structural information of these binary and ternary Np(VI) (hydr)oxide phases were reported in [8–10]). Furthermore, clear evidence was found in [4] that the monomeric complexes  $\text{NpO}_2(\text{OH})_3^-$  and  $\text{NpO}_2(\text{OH})_4^{2-}$  are the predominant Np(VI) species in equilibrium with the Np(VI) solid phases under alkaline pH conditions. Comprehensive chemical and thermodynamic data were derived showing that Np(VI) has a qualitatively similar solubility behavior as U(VI) in alkaline NaCl media. Additional structural information about the limiting hydrolysis complexes of Np(VI) in strongly alkaline solutions with  $[\text{OH}^-] \geq 0.5 \text{ mol dm}^{-3}$  were provided by, e.g., Williams et al. (EXAFS,  $1 \text{ mol dm}^{-3}$  NaOH), Bolvin et al. (EXAFS and DFT,  $2.5 \text{ mol dm}^{-3}$  NaOH), Gaona et al. (EXAFS,  $0.5 \text{ mol dm}^{-3}$ , TMAOH) and Clark et al. (EXAFS, single crystal XRD, Raman,  $0.5\text{--}3.5 \text{ mol dm}^{-3}$  LiOH, NaOH, TMAOH) [11–14]. According to these authors, Np(VI) exists dominantly as the symmetric sixfold coordinated  $\text{NpO}_2(\text{OH})_4^{2-}$  under strongly alkaline conditions ( $0.5 \text{ mol dm}^{-3} \leq [\text{OH}^-] \leq 3.5 \text{ mol dm}^{-3}$ ). Indications were found for the formation of a penta-hydroxo complex  $\text{NpO}_2(\text{OH})_5^{3-}$  at greater alkalinity ( $[\text{OH}^-] \geq 3.5 \text{ mol dm}^{-3}$ ).

Over the last decade, we have systematically investigated the solubility behavior and thermodynamics of actinides, and selected lanthanides (Ln) and transition metals (M) in alkaline  $\text{CaCl}_2$  [and to a lesser extent in  $\text{Ca}(\text{ClO}_4)_2$ ] solutions, namely of Cm(III), Nd(III), Th(IV), Np(IV), Pu(IV), Tc(IV), Zr(IV), Np(V), U(VI) [15–21]. These comprehensive results revealed significant differences in the aqueous and solid speciation of these elements for alkaline  $\text{CaCl}_2$  ( $\text{Ca}(\text{ClO}_4)_2$ ) solutions compared to the well-studied behavior in neutral to alkaline NaCl ( $\text{NaClO}_4$ ) solutions of similar ionic strength, alkalinity, and chloride concentration [1]. For example, in  $\text{CaCl}_2$  solutions with  $\text{pH}_m = -\log\{m(\text{H}^+)/\text{mol}(\text{kg H}_2\text{O})^{-1}\} > 10$ , the predominant hydrolysis species of An(III)/Ln(III), An(IV)/M(IV), and An(V) are Ca-stabilized, ternary Ca–An–OH complexes with significantly greater number of hydroxo ligands compared to the binary An–OH (Ln–OH, M–OH) complexes forming in Na-dominated solutions of similar  $\text{pH}_m$  values, e.g.,  $\text{Ca}_3[\text{Cm}^{\text{III}}(\text{OH})_6]^{3+}$  vs.  $\text{Cm}^{\text{III}}(\text{OH})_3(\text{aq})$ ,  $\text{Ca}_4[\text{An}^{\text{IV}}(\text{OH})_8]^{4+}$  vs.  $\text{An}^{\text{IV}}(\text{OH})_4(\text{aq})$ , and  $\text{Ca}_3[\text{Np}^{\text{V}}\text{O}_2(\text{OH})_5]^{2+}$  vs.  $\text{Np}^{\text{V}}\text{O}_2(\text{OH})_2^-$ . The Ca-specific complexes lead to a pronounced stabilization of the aqueous An (Ln/M) speciation and, accordingly, to enhanced solubility in alkaline  $\text{Ca}^{2+}$  containing solutions. Analogous Ca–An(VI)–OH species are not yet reported. Furthermore, the relevance of Ca-containing An(V) and An(VI)

(hydr)oxides like calcium neptunate(V) Ca<sub>0.5</sub>Np<sup>V</sup>O<sub>2</sub>(-OH)<sub>2</sub>(cr,hyd), becquerelite CaU<sub>6</sub>O<sub>9</sub>·11H<sub>2</sub>O(cr) or calcium uranate(VI) CaU<sub>2</sub>O<sub>7</sub>(cr,hyd) as solubility limiting An solid phases was established, and their solubility and thermodynamics analyzed [21–24]. Compared to the corresponding binary An solid phases, NpO<sub>2</sub>OH(am) and metaschoepite UO<sub>3</sub>·2H<sub>2</sub>O(cr), the ternary compounds are significantly more stable, i.e., less soluble, in neutral to alkaline Ca<sup>2+</sup> containing solutions.

To the best of our knowledge, no systematic study on the solution chemistry of Np(VI) in alkaline CaCl<sub>2</sub> solution has been reported. As an extension of our previous work on Np(IV) and Np(V), we have therefore investigated the solubility, speciation and solid phase formation of Np(VI) in alkaline 0.25–4.5 mol dm<sup>-3</sup> CaCl<sub>2</sub> solutions [17, 19, 20]. This work offers interesting new data on scientifically challenging systems and allows one to draw comparisons along the An(VI) series, notably U(VI).

## Results and discussion

### Characterization of the solubility controlling Np(VI) solid phases

As detailed in the “[Experimental](#)”, the initial Np(VI) solid phase used for the solubility experiments (discussed in the subsequent section) was obtained as a precipitate by alkalization of an electrochemically prepared acidic Np(VI) stock solution with concentrated, alkaline CaCl<sub>2</sub> solution. The final conditions of the mother liquor were [CaCl<sub>2</sub>] = 4.2 mol dm<sup>-3</sup> and pH<sub>m</sub> 11.2.

The results of the solid phase analyses of the Np(VI) starting material, as well as of equilibrium solid phases retrieved from additional 16 batch samples at the end of the solubility study are summarized in Table 1.

The XRD pattern of the initial Np(VI) precipitate consists of few, relatively broad peaks pointing to a poorly crystalline compound, see Fig. 1. It does apparently not match the ones of the well-defined, microcrystalline compounds NpO<sub>2</sub>(OH)<sub>2</sub>·H<sub>2</sub>O(cr), Na<sub>2</sub>Np<sub>2</sub>O<sub>7</sub>(cr), and CaU<sub>2</sub>O<sub>7</sub>·3H<sub>2</sub>O(cr), which control the An(VI) solubility in alkaline NaCl (Np) and CaCl<sub>2</sub> (U) solutions, respectively [4, 21]. SEM analysis (Fig. 2) shows that the Np(VI) solid consists of relatively large agglomerated particles (overall agglomeration size up to 30 μm) without a defined microstructure, which is in line with its poorly crystalline nature indicated by the XRD pattern. Quantitative chemical analysis of the (dissolved) initial Np(VI) precipitate by ICP-OES and LSC revealed a ratio Ca:Np = 1.28:1 and confirms the formation of a calcium containing Np(VI) solid compound. EDX analysis further corroborates the presence of structural calcium (ratio Ca:Np ≈ 1:1). Based

on the more precise combined OES and LSC chemical analyses, the overall formula Ca<sub>1.28</sub>NpO<sub>4.28</sub>(s,hyd) is estimated (notation as oxide was chosen in analogy to the oxidic nature of most An(VI) compounds, especially with the formula reported for sodium polyuranate Na<sub>x</sub>UO<sub>(3+x/2)</sub>(s,hyd) [25]. From the experimental data it can, however, not be decided if the Ca–Np(VI) solid phase of the present work is a pure oxide, a pure hydroxide, or mixed oxide-hydroxide).

A quantitative chemical analysis of selected solid phases from the batch solubility samples discussed in the next section was conducted by combined ICP-OES (Ca) and LSC (Np) after *t* ≈ 200 days (in most cases). At this time, stable values for [Np] and pH<sub>m</sub> had been attained. While no changes in the appearance (e.g., color) could be visually observed, the results of chemical analyses clearly showed that the overall solid phase stoichiometry had changed, pointing to a transformation of the initial Ca<sub>1.28</sub>NpO<sub>4.28</sub>(s,hyd) under the specific solution conditions of the solubility samples. Values determined for the structural Ca:Np ratio ranged between 0.60:1 and 1.66:1, i.e., a transformation occurred towards lower and higher calcium contents with respect to the Np(VI) starting compound.

As shown in Fig. 3, the Ca:Np solid phase ratios were systematically correlated to the pH<sub>m</sub> values of the batch samples: the higher the pH<sub>m</sub>, the higher the Ca-content in the solid phase. Interestingly, there was no apparent correlation with the CaCl<sub>2</sub> concentration of the solubility samples. While the highest Ca-content could be expected in the solid equilibrated at the highest [CaCl<sub>2</sub>] = 4.5 mol dm<sup>-3</sup> (and highest pH<sub>m</sub> 11.6), it was found for the solid phase equilibrated in 0.25 mol dm<sup>-3</sup> CaCl<sub>2</sub> solutions (and highest pH<sub>m</sub> 12.0). Although solid phases from samples with [CaCl<sub>2</sub>] = 1.0 and 3.5 mol dm<sup>-3</sup> were not analyzed, it is expected that they follow the same trend with pH<sub>m</sub>.

Several of the 16 solid samples mentioned before were also analyzed by powder XRD, c.f. Table 1 and Fig. 1. As for the initial material, the patterns show only a limited number of broad peaks which corroborate the presence of poorly crystalline solid phases (the sharp peaks observed in the sample with [CaCl<sub>2</sub>] = 0.25 mol dm<sup>-3</sup> and pH<sub>m</sub> 12.0 can be assigned to portlandite precipitation). Practically none of the patterns perfectly match exactly the other, which is somehow in line with the continuously changing stoichiometry. Most of the Ca–Np(VI) solid samples show more than one peak in the principal region 2θ ≈ 5–20. Their positions in the various patterns are at 2θ ≈ 8.9, 2θ ≈ 9.9, 2θ ≈ 11.8, 2θ ≈ 12.4, 2θ ≈ 12.8, 2θ ≈ 13.1, and 2θ ≈ 13.6. In the case of the stoichiometric, crystalline CaU<sub>2</sub>O<sub>7</sub>·3H<sub>2</sub>O(cr), Na<sub>2</sub>Np<sub>2</sub>O<sub>7</sub>(cr) and NpO<sub>2</sub>(OH)<sub>2</sub>·H<sub>2</sub>O(cr) only one peak at 2θ ≈ 13.9, 15.0, and 12.4, respectively, is observable in this region. This

**Table 1** Summary of solid phase characterizations conducted with the initial Np(VI) solid precipitate and equilibrium solid phases retrieved from batch solubility samples after  $\approx 200$  days (in most cases)

Sample: [CaCl <sub>2</sub> ] mol dm <sup>-3</sup> /pH <sub>m</sub>	Ca:Np ratio	Stoichiometry (see text)	Additional analysis	
4.2 <sup>a</sup>	11.2	1.28:1	Ca <sub>1.28</sub> NpO <sub>4.28</sub> (s,hyd)	SEM-EDX, XRD
0.25	8.9	0.67:1	Ca <sub>0.67</sub> NpO <sub>3.67</sub> (s,hyd)	
0.25	9.7	0.74:1	Ca <sub>0.74</sub> NpO <sub>3.74</sub> (s,hyd)	XRD
0.25	10.1	0.85:1	Ca <sub>0.85</sub> NpO <sub>3.85</sub> (s,hyd)	
0.25	10.6	1.04:1	Ca <sub>1.04</sub> NpO <sub>4.04</sub> (s,hyd)	
0.25	11.1	1.19:1	Ca <sub>1.19</sub> NpO <sub>4.19</sub> (s,hyd)	XRD
0.25	11.5	1.38:1	Ca <sub>1.38</sub> NpO <sub>4.38</sub> (s,hyd)	
0.25	12.0	1.66:1	Ca <sub>1.66</sub> NpO <sub>4.66</sub> (s,hyd)	XRD
2.0	8.8	0.60:1	Ca <sub>0.60</sub> NpO <sub>3.60</sub> (s,hyd)	
2.0	9.3	0.67:1	Ca <sub>0.67</sub> NpO <sub>3.67</sub> (s,hyd)	XANES, XRD
2.0	9.7	0.81:1	Ca <sub>0.81</sub> NpO <sub>3.81</sub> (s,hyd)	
2.0	10.3	1.01:1	Ca <sub>1.01</sub> NpO <sub>4.01</sub> (s,hyd)	
2.0	10.8	1.25:1	Ca <sub>1.25</sub> NpO <sub>4.25</sub> (s,hyd)	XRD
2.0	11.3	1.39:1	Ca <sub>1.39</sub> NpO <sub>4.39</sub> (s,hyd)	
2.0	11.8	1.58:1	Ca <sub>1.58</sub> NpO <sub>4.58</sub> (s,hyd)	XANES, XRD
4.5	10.1	1.09:1	Ca <sub>1.09</sub> NpO <sub>4.09</sub> (s,hyd)	XRD
4.5	11.6	1.43:1	Ca <sub>1.43</sub> NpO <sub>4.43</sub> (s,hyd)	XRD

The Ca:Np ratios in the solid phase structure were determined by combined ICP-OES and LSC analyses. The absolute uncertainty in the Ca and Np determination is estimated as 5% each

<sup>a</sup>Initial Np(VI) material

suggest that the solid phase properties of the system Np(VI) in alkaline CaCl<sub>2</sub> solutions are apparently highly complex. The XRD patterns reveal a large number of different phase compositions or “chain members” which might be explained by the formation of one or more Ca–Np(VI)-(hydr)oxide solid solutions. The fact that the Ca:Np ratios are not fully correlated with the peak positions in the powder XRD patterns further underlines the apparent complexity of the system (considering the rather poor quality, i.e., intensities of the patterns, an over-interpretation of the powder XRD data should be avoided). In none of the XRD patterns peaks of the very stable, microcrystalline Ca–Np(V)-hydroxide phases reported in [19], namely Ca<sub>0.5</sub>NpO<sub>2</sub>(OH)<sub>2</sub>·1.3H<sub>2</sub>O(s), Ca<sub>0.5</sub>NpO<sub>2</sub>(OH)<sub>2</sub>(s), and CaNpO<sub>2</sub>(OH)<sub>2.6</sub>Cl<sub>0.4</sub>·2H<sub>2</sub>O(s), were observed which clearly corroborates the absence of Np(V) in the solid phases of the present work.

The equilibrium solid phases from the solubility samples in 2.0 mol dm<sup>-3</sup> CaCl<sub>2</sub> with pH<sub>m</sub> 9.3 and 11.8 were studied by Np L3-edge XANES. The positions of the first inflection points  $E_{ip}$  as well as the white-line maxima  $E_{max}$  of the XANES spectra (Fig. 4) at 17,611.0 and 17,617.0 eV (pH<sub>m</sub> 9.3) and 17,610.4 and 17,617.2 eV (pH<sub>m</sub> 11.8), respectively, are comparable with solid and aqueous Np(VI) species reported in [7] with  $E_{ip} = 17,609.3$ – $17,610.2$  eV and  $E_{max} = 17,615.5$ – $17,616.6$  eV and clearly confirm presence of hexavalent Np in the solid phase. As a comparison, XANES data for three solid Np(V) hydroxide

compounds investigated in our related study are in the ranges  $E_{ip} = 17,607.4$ – $17,609.8$  eV and  $E_{max} = 17,613.4$ – $17,614.0$  eV, respectively, i.e., significantly different from the present Np(VI) data [19].

Np L3-XANES white-line (WL) features, i.e., the obvious dampening and broadening and the energy shift of the axial multiple scattering feature towards the peak maximum compared to neptunyl species (giving the typical WL appearance of a skewed plateau), unambiguously indicate the presence of a neptunate structure (with elongated axial oxygen and reduced average equatorial oxygen distances), c.f. [26].

The results of the solid phase characterizations clearly indicate that non-stoichiometric Ca–Np(VI)-(hydr)oxide compounds with variable Ca:Np solid ratio, the latter being strongly correlated to the solution pH<sub>m</sub>, control the solubility of Np(VI) in the alkaline CaCl<sub>2</sub> solutions of the present work rather than a distinct (stoichiometric) solid phase. Similar behavior was reported for U(VI) solubility in NaCl and NaClO<sub>4</sub> solutions under near-neutral pH conditions, where sodium containing uranyl-oxyhydrate solid solutions (sodium polyuranates) Na<sub>x</sub>UO<sub>(3+x/2)</sub>(s,hyd) with variable Na:U ratios (e.g., going from 0.11:1 to 0.68:1 in 5 mol dm<sup>-3</sup> NaCl) were identified as solubility controlling solid phases [25]. In analogy, the Np(VI) solids of the present work can be described as calcium neptunates, Ca<sub>x</sub>NpO<sub>3+x</sub>(s,hyd), with experimentally observed values for  $x$  ranging from 0.60 to 1.66, c.f. Table 1. Although no

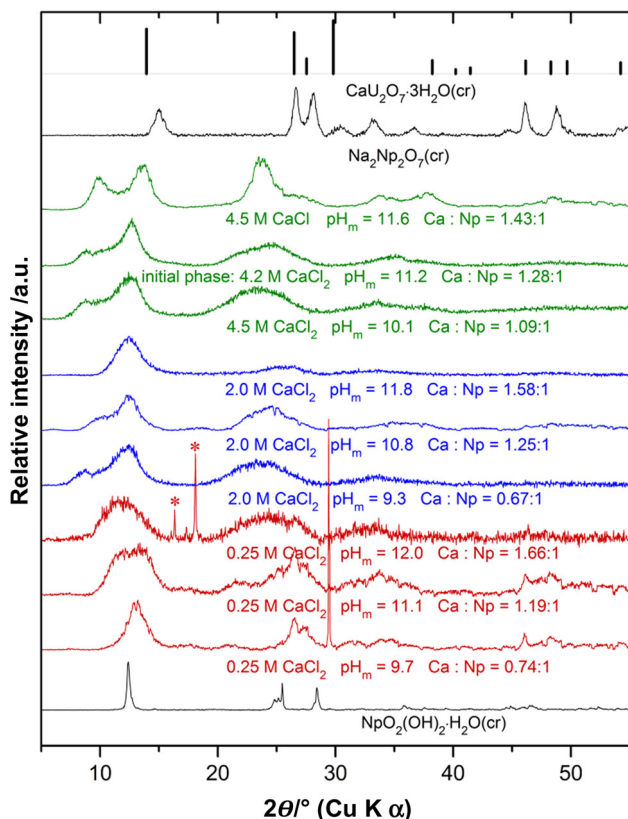


**Fig. 1** Powder XRD patterns of the calcium containing Np(VI) solid phases of the present work. Reference spectra of binary  $\text{NpO}_2(\text{OH})_2 \cdot \text{H}_2\text{O}(\text{cr})$  and ternary  $\text{Na}_2\text{Np}_2\text{O}_7(\text{cr})$  and  $\text{CaU}_2\text{O}_7 \cdot 3\text{H}_2\text{O}(\text{cr})$  are shown as comparison [4, 21]. Presence of sharp peaks marked by asterisks are explained in the text

specific determination of the degree of hydration water was performed, e.g., by thermogravimetric analysis, it is likely that the Np(VI) solids contain a certain degree of water indicated by “hyd” due to its rather poorly crystalline characteristics. The various stoichiometries of the calcium neptunates (based on the chemical analysis) may represent

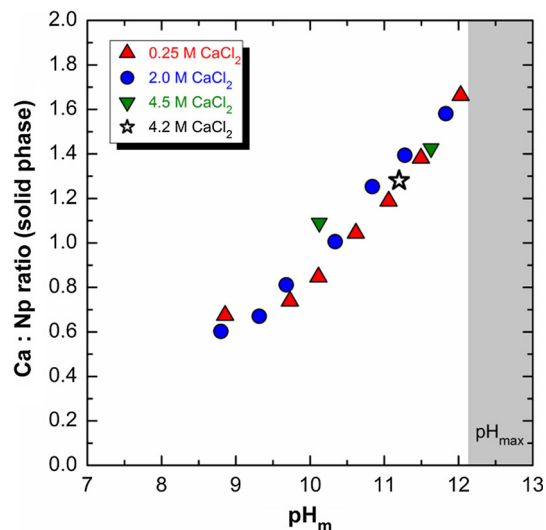


**Fig. 3** Experimentally determined Ca:Np ratio in the equilibrium solid phase of several batch solubility samples. A ratio Ca:Np = 1.28:1 was determined in the initial Np(VI) compound (equilibrated in 4.2 mol dm<sup>-3</sup> CaCl<sub>2</sub> and  $\text{pH}_m$  11.2, marked as star symbol)

members of one or more solid solutions, with the potential endmembers  $\text{Ca}_{0.5}\text{NpO}_{3.5}(\text{s},\text{hyd})$  and  $\text{Ca}_2\text{NpO}_5(\text{s},\text{hyd})$ .

The findings of the present work clearly differ from the solution behavior reported for Np(VI) in alkaline NaCl and U(VI) in alkaline NaCl and CaCl<sub>2</sub> solutions where stoichiometric, microcrystalline solid phases,  $\text{AnO}_2(\text{OH})_2 \cdot x\text{H}_2\text{O}(\text{cr})$ ,  $\text{Na}_2\text{An}_2\text{O}_7 \cdot x\text{H}_2\text{O}(\text{cr})$  with An = Np, U and  $\text{CaU}_2\text{O}_7 \cdot 3\text{H}_2\text{O}(\text{cr})$  control the solubility over wide ranges of  $\text{pH}_m$  conditions and electrolyte concentrations [4, 21, 27].

### Batch solubility experiments

The results of the previous section indicate that Np(VI) solubility in the various alkaline CaCl<sub>2</sub> solutions was controlled by  $\text{Ca}_x\text{NpO}_{3+x}(\text{s},\text{hyd})$  with  $x = 0.60:1-1.66:1$

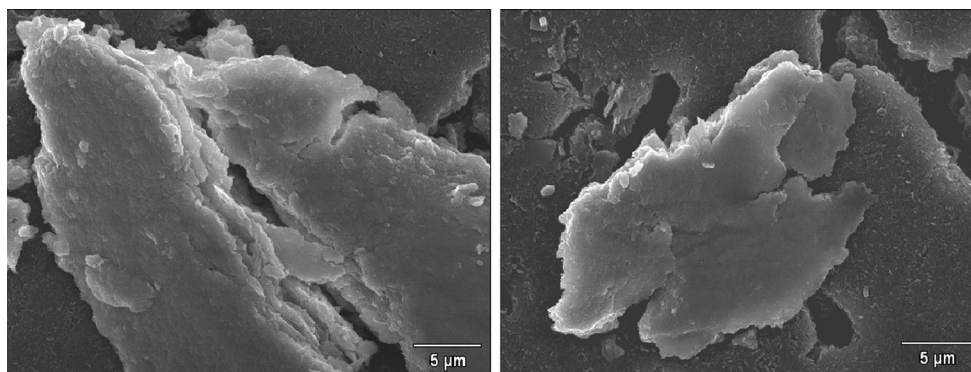


**Fig. 2** Scanning electron microscope pictures of the initial Np(VI) solid phase  $\text{Ca}_{1.28}\text{NpO}_{4.28}(\text{s},\text{hyd})$

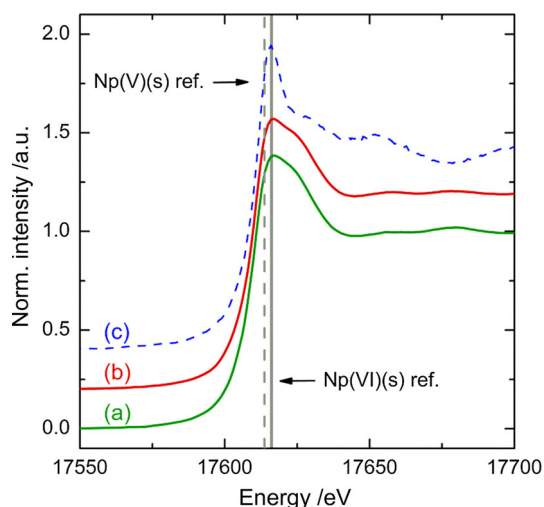


**Fig. 4** Experimental Np L3-edge XANES spectra of two solid phases retrieved from solubility samples in  $2.0 \text{ mol dm}^{-3}$   $\text{CaCl}_2$  at  $\text{pH}_m$  11.8 (a), and  $\text{pH}_m$  9.3 (b) of the present work in comparison to aqueous  $\text{NpO}_2^{2+}$  in  $1 \text{ mol dm}^{-3}$   $\text{HClO}_4$  (c), solid Np(VI) reference samples (position of  $E_{\text{max}}$  indicated as grey solid line) and solid Np(V) reference samples (position of  $E_{\text{max}}$  indicated as grey dashed line) from [7, 19]

which readily formed under the individual solution conditions from the initially added  $\text{Ca}_{1.28}\text{NpO}_{4.28}(\text{s},\text{hyd})$ .

#### Main series with $[\text{CaCl}_2] = 0.25\text{--}4.5 \text{ mol dm}^{-3}$ and $[\text{NaOCl}] = 5 \times 10^{-3} \text{ mol dm}^{-3}$

To establish highly oxidizing solution conditions,  $5 \times 10^{-3} \text{ mol dm}^{-3}$   $\text{NaOCl}$  was used as the oxidizing agent for the main series. During the entire period of the study, measured redox potentials  $\text{pe} = 16.9 \times E_h$  were more than 3.5 pe-units above the upper decomposition line of water (defined as  $\text{pe} + \text{pH} = 20.8$  for dilute solutions), see Fig. 5, which is sufficient to stabilize Np(VI) based on the results reported in [4, 7]. Under comparable  $\text{pH}_m$  conditions, the experimental pe values increased systematically with increasing  $[\text{CaCl}_2]$ , which can qualitatively be explained by the changing activities of solution species at greater  $[\text{CaCl}_2]$ .

The solubility data of calcium neptunates in  $0.25\text{--}4.5 \text{ mol dm}^{-3}$   $\text{CaCl}_2$  solutions at  $\text{pH}_m$  8.5–12.0 is displayed in Fig. 6a–e. Note that the molal values for  $\log [\text{Np}]$  and  $\text{pH}_m$  are displayed in all figures throughout the manuscript, whereas the corresponding molar values are typically used in the text for better readability. While slight changes of the Np(VI) solubility occurred especially within the first two samplings ( $t < 49$  days to  $t < 62$  days; these data are not shown in the graph, but are provided as electronic supplementary material), presumably caused by the time evolution of the initial to the final solid phase composition (calcium content), stable Np(VI) equilibrium

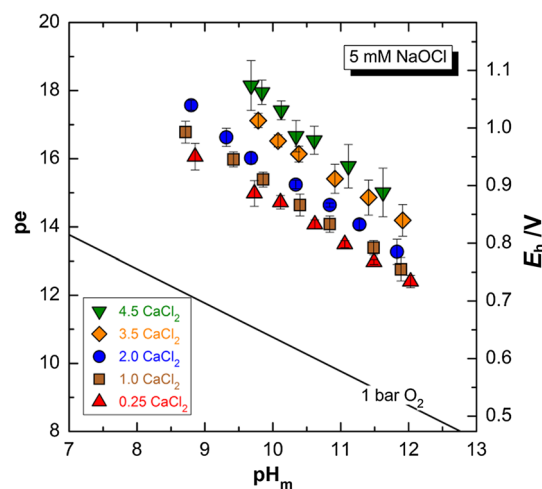
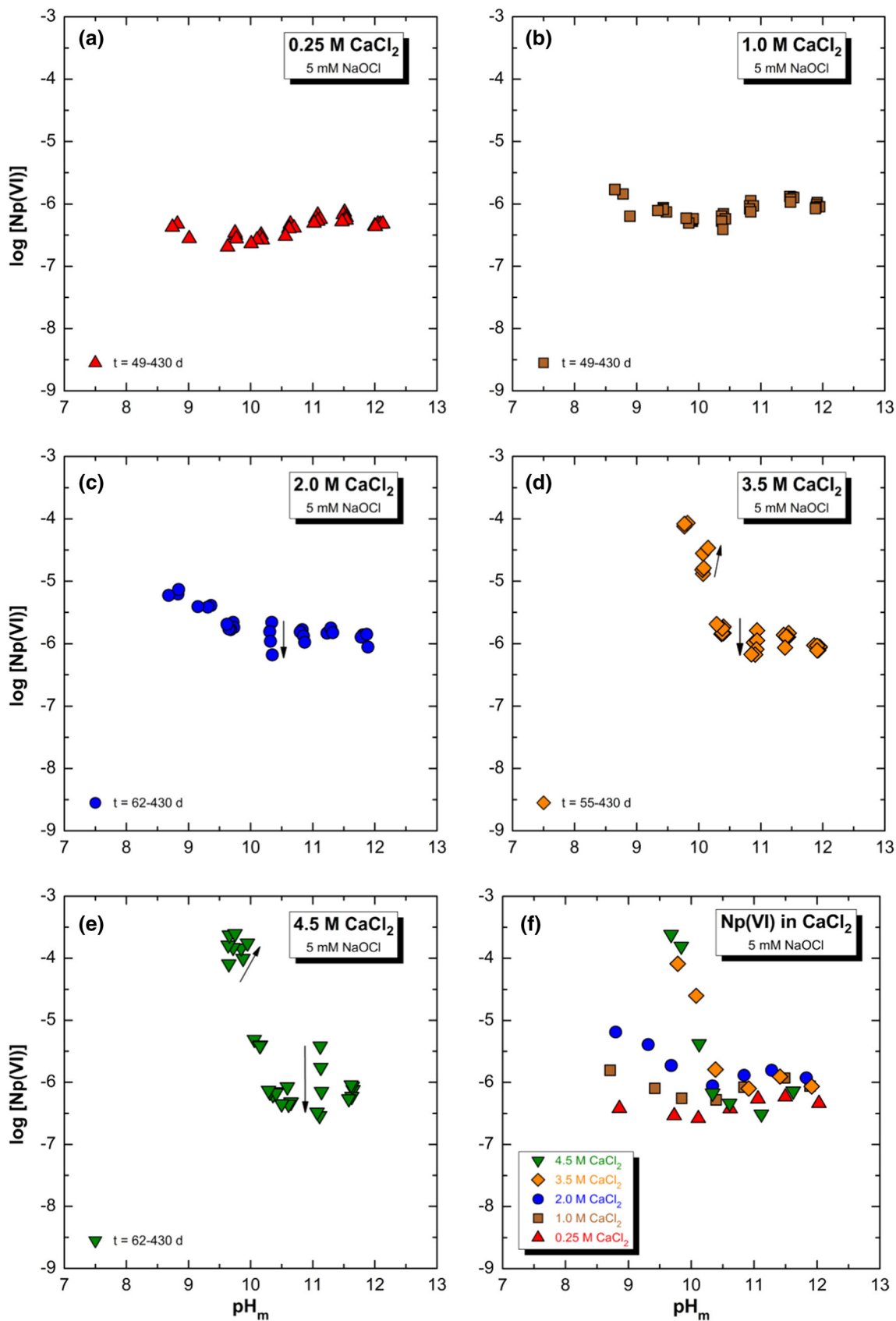


**Fig. 5** Mean values of the redox potentials  $\text{pe} = 16.9 \times E_h$  measured in the Np(VI) batch samples with  $[\text{CaCl}_2] = 0.25\text{--}4.5 \text{ mol dm}^{-3}$  (standard deviation given as error bars), which were without exception more than 3.5 pe-units above the upper decomposition line of water

**Fig. 6 a–e** Experimental molal solubility of  $\text{Ca}_x\text{NpO}_{3+x}(\text{s},\text{hyd})$  with  $x = 0.60\text{--}1.66$  in  $0.25\text{--}4.5 \text{ mol dm}^{-3}$   $[\text{CaCl}_2]$  solutions of the main series with  $[\text{NaOCl}] = 5 \times 10^{-3} \text{ mol dm}^{-3}$ , c.f. Table 1. The data of the first two samplings are not displayed, but are provided as electronic supplementary material, see text. Arrows indicate samples showing an apparent drift for up to  $t \approx 200$  days. **f** Comparison of the stable solubility data of the different series (i.e., mean values of several samplings for most of the samples)

concentrations were typically found for  $t \approx 60\text{--}430$  days [estimated uncertainties of  $\text{pH}_m$  and  $\log [\text{Np}]$  are about 0.04 and 0.05–0.15 (depending on the sample), respectively]. Few samples showing an apparent drift with time for  $t > 60$  days are marked by an arrow in Fig. 6a–e, but even for these few cases, the last two samplings at  $t \approx 200$  days (where the re-analysis of the batch solid phases was performed) and  $t \approx 430$  days showed practically the same solubility data, i.e., equilibrium between respective solid and liquid state was attained. Stable  $\log [\text{Np}]$  and  $\text{pH}_m$  data (average values for most of the samples) obtained for the five series are compared in Fig. 6f.

The experimental solubility curve of  $\text{Ca}_x\text{NpO}_{3+x}(\text{s},\text{hyd})$  in  $0.25\text{--}4.5 \text{ mol dm}^{-3}$   $\text{CaCl}_2$  solutions can be divided into two general regions: in more alkaline solutions with  $\text{pH}_m > 10.5$ , the solubility is around  $\log [\text{Np}] \approx -6.1 \pm 0.4$ , without showing a strong dependence on  $[\text{CaCl}_2]$  despite the considerably changing concentration of the latter. On the other hand, for  $\text{pH}_m < 10.5$  the experimental solubility curve,  $\log [\text{Np}]$  vs.  $\text{pH}_m$ , are well represented by straight lines with slopes going from  $-1/4$  in  $0.25 \text{ mol dm}^{-3}$   $\text{CaCl}_2$  to  $-4$  in  $4.5 \text{ mol dm}^{-3}$   $\text{CaCl}_2$ , i.e., becoming



steeper with increasing  $[\text{CaCl}_2]$ . In 3.5 and 4.5 mol dm<sup>-3</sup>  $\text{CaCl}_2$  solutions, this leads to a relatively great Np solubility of  $\log [\text{Np}] \approx -4.0 \pm 0.5$  around  $\text{pH}_m$  10, while  $\log [\text{Np}] < -5.0$  for the less concentrated solutions and  $\text{pH}_m > 8.5$ . The experimental solubility data are used to qualitatively evaluate the predominant equilibrium reactions, see “Discussion”.

**Additional series with  $[\text{CaCl}_2] = 0.25$   
and 2.0 mol dm<sup>-3</sup>  
and  $[\text{NaOCl}] = 5 \times 10^{-4}$  mol dm<sup>-3</sup>  
and  $5 \times 10^{-2}$  mol dm<sup>-3</sup>**

Pashalidis et al. reported the formation of Pu(VI) hypochlorito complexes,  $\text{PuO}_2(\text{OH})(\text{ClO})(\text{aq})$  and  $\text{PuO}_2(-\text{ClO})_2(\text{aq})$ , in 5 mol dm<sup>-3</sup> NaCl solutions and near-neutral pH conditions in presence of  $[\text{OCl}^-] = 0.2\text{--}0.55$  mol dm<sup>-3</sup> [28]. On the other hand, Gaona et al. did not observe significant effects of  $[\text{OCl}^-] = 5 \times 10^{-3}$  mol dm<sup>-3</sup> on the Np(VI) solubility in hyperalkaline 0.1 and 5.0 mol dm<sup>-3</sup> NaCl solutions, but indicated a potential effect at greater  $[\text{OCl}^-]$  [4]. To test a potential impact of NaOCl on the Np(VI) speciation in  $\text{CaCl}_2$  solutions, an additional series of seven samples was investigated in the present work, with ten times higher and lower  $[\text{NaOCl}]$  compared to the main series, respectively. Figure 7 displays the experimental solubility data in 0.25 and 2.0 mol dm<sup>-3</sup>  $\text{CaCl}_2$  as function of the NaOCl concentration.

Except for the sample with  $[\text{CaCl}_2] = 0.25$  mol dm<sup>-3</sup> and  $\text{pH}_m$  10, where the solubility is enhanced by a factor of 2 (i.e., 0.3 log-units) upon an increase of  $[\text{NaOCl}]$  by a factor of 100 (i.e., 2 log-units), no significant changes of the solubility with varying  $[\text{NaOCl}]$  were found. Independent, if the one exception represents a real trend—then its impact at this  $\text{pH}_m$  is low and apparently becomes insignificant with increasing  $\text{pH}_m$  and  $[\text{CaCl}_2]$ —it can still be robustly stated, that Np(VI)

hypochlorito complexes did not significantly influence the solubility data of the main experimental series with  $[\text{NaOCl}] = 5 \times 10^{-3}$  mol dm<sup>-3</sup>. Note that for  $[\text{CaCl}_2] = 2.0$  mol dm<sup>-3</sup> no effect is observed even at lower  $\text{pH}_m$  9.0. This may indicate that the slightly enhanced Np solubility in 0.25 mol dm<sup>-3</sup>  $\text{CaCl}_2$  at  $\text{pH}_m$  10 is rather an effect of the changing matrix; the content of  $\text{Na}^+$  relative to  $\text{Ca}^{2+}$  increases from 0.2 to 20% which represents an important change in the matrix composition.

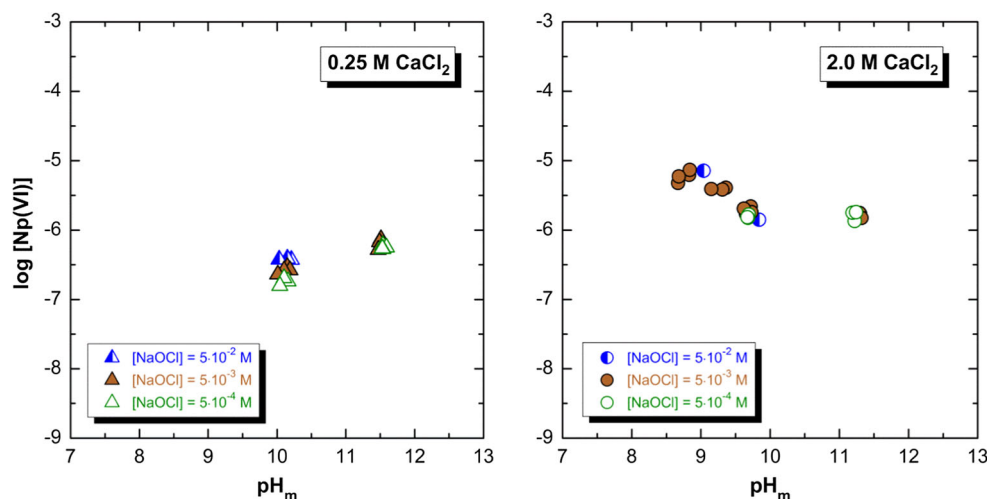
As expected, measured redox potentials systematically increased with higher  $[\text{NaOCl}]$  for the same  $[\text{CaCl}_2]$  and  $\text{pH}_m$  conditions, and followed nearly Nernstian behavior (e.g., for  $[\text{CaCl}_2] = 2.0$  mol dm<sup>-3</sup> with  $\text{pH}_m$   $9.8 \pm 0.1$ ,  $\text{pe} = 15.3 \pm 0.1/16.0 \pm 0.2/17.0 \pm 0.1$  for  $[\text{NaOCl}] = 5 \times 10^{-4}/5 \times 10^{-3}/5 \times 10^{-2}$  mol dm<sup>-3</sup>). The absence of changes in the total Np solubility at various  $[\text{NaOCl}]$ , i.e., under various pe conditions in the range  $\pm 1$  pe-units at the same  $\text{pH}_m$ , further corroborates the absence of significant amounts of other Np oxidation states, especially Np(V), both in the solid and liquid phase, as this would directly depend on the pe conditions.

#### UV-Vis/NIR investigations

The supernatant solutions of two solubility samples in 4.5 mol dm<sup>-3</sup>  $\text{CaCl}_2$  with final  $\text{pH}_m$  9.68 and 9.84 showing the greatest overall Np concentration of the present study were analyzed by UV-Vis/NIR spectroscopy at  $t = 151$  days (for which  $[\text{Np}]_{\text{tot}} = 2.03 \times 10^{-4}$  and  $1.24 \times 10^{-4}$  mol dm<sup>-3</sup>, respectively). The NIR region of the spectra ( $\lambda = 900\text{--}1300$  nm) is displayed in Fig. 8, the UV-Vis region ( $\lambda = 300\text{--}800$  nm) in Fig. 9, the latter showing significantly greater absorption intensities (note the different scales of the y-axes).

While the prominent Vis/NIR peak of the  $\text{NpO}_2^{2+}$  aquo ion in 2 mol dm<sup>-3</sup>  $\text{HClO}_4$  is at  $\lambda \approx 1223$  nm with

**Fig. 7** Experimental molal solubility of  $\text{Ca}_x\text{NpO}_{3+x}(\text{s,hyd})$  in 0.25 and 2.0 mol dm<sup>-3</sup>  $[\text{CaCl}_2]$  solutions with  $[\text{NaOCl}] = 5 \times 10^{-4}$  (open symbols) and  $5 \times 10^{-2}$  mol dm<sup>-3</sup> (half-open symbols) of the additional series in comparison to the data of the main series with  $[\text{NaOCl}] = 5 \times 10^{-3}$  mol dm<sup>-3</sup> (closed symbols)





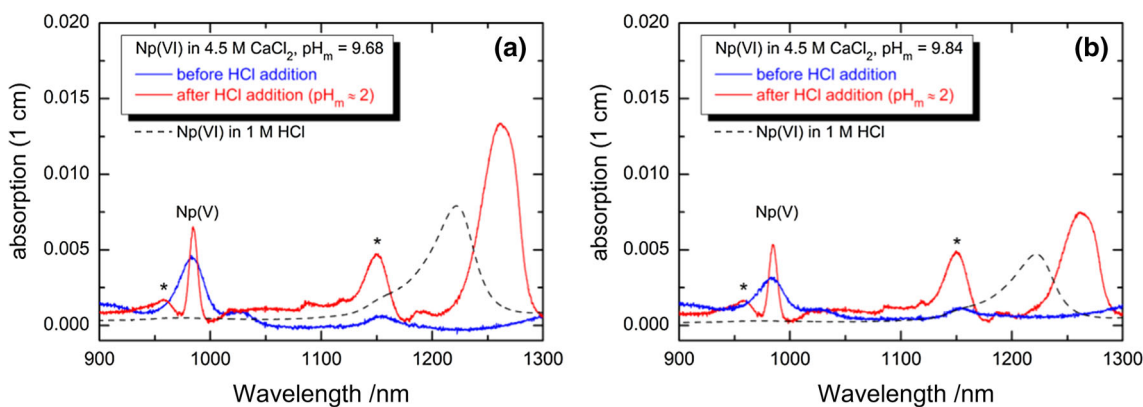


**Fig. 8** NIR spectra of supernatant solutions of two Np(VI) solubility samples in 4.5 mol dm<sup>-3</sup> CaCl<sub>2</sub> with (a) pH<sub>m</sub> 9.68 and (b) pH<sub>m</sub> 9.84 of the main series with [NaOCl] = 5 × 10<sup>-3</sup> mol dm<sup>-3</sup>. Spectra obtained for the original solutions are compared to the ones recorded of the corresponding acidified aliquots (pH<sub>m</sub> ≈ 2) after addition of few microliters of HCl. The asterisks mark the absorption feature of

water (baseline mismatch), as discussed in the text. The dashed line represents the spectrum of the electrochemically prepared Np(VI) stock solution in 1 mol dm<sup>-3</sup> HCl (see “Experimental”) normalized to the same Np(VI) concentration as present in the two solubility samples

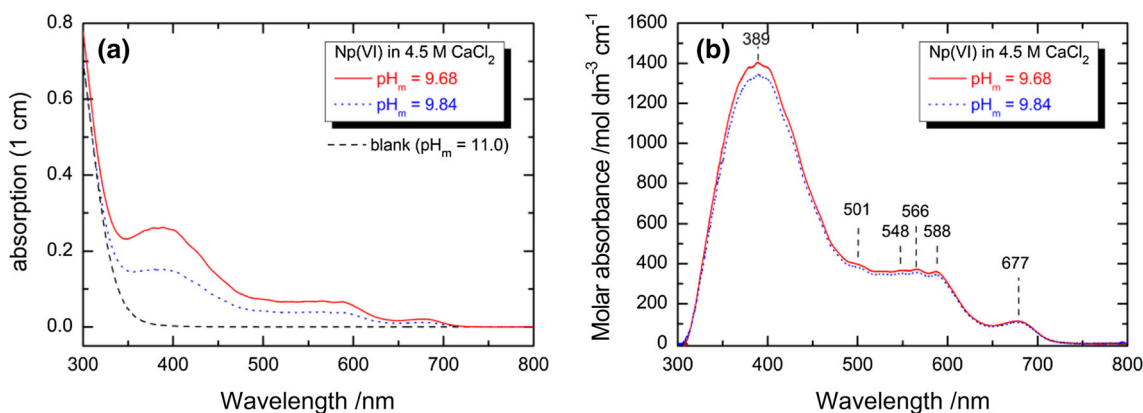


**Fig. 9** UV-Vis spectra of supernatant solutions of two Np(VI) solubility samples in 4.5 mol dm<sup>-3</sup> CaCl<sub>2</sub> with pH<sub>m</sub> 9.68 and 9.84 of the main series with [NaOCl] = 5 × 10<sup>-3</sup> mol dm<sup>-3</sup> highlighting the more intensive features: **a** original spectra compared to spectrum of Np-free 5 × 10<sup>-3</sup> mol dm<sup>-3</sup> NaOCl in 4.5 mol dm<sup>-3</sup> CaCl<sub>2</sub> with

pH<sub>m</sub> 11.0 (“blank”) and **b** residual spectra of predominant Np(VI) species after subtraction of absorption peaks of the NaOCl system (“blank”). Spectra are normalized for [Np(VI)] = [Np]<sub>tot</sub> - [Np(V)], the latter being determined from spectra of the corresponding acidified sample aliquots, c.f. Fig. 8

$\epsilon \approx 43 \text{ dm}^{-3} \text{ mol}^{-1} \text{ cm}^{-1}$ , no absorption around this wavelength region is observed in the spectra of the two alkaline sample aliquots, see Fig. 8 [29]. Note that the peak at  $\lambda \approx 1150 \text{ nm}$  with Abs  $\approx 0.001$  is identified as the NIR absorption of water, and is also present in the spectrum of the Np-free “blank solution” with [NaOCl] = 5 × 10<sup>-3</sup> mol dm<sup>-3</sup> in 4.5 mol dm<sup>-3</sup> CaCl<sub>2</sub> and pH<sub>m</sub> ≈ 11.0 (caused by a baseline mismatch due to slightly differing contents of free water and likewise the [CaCl<sub>2</sub>] in the reference and the corresponding sample cuvette). The absence of an apparent NIR absorption of Np(VI) indicates that the spectral NIR feature of the predominant Np(VI) species—expectedly a hydrolysis species—are either red-shifted beyond the measured wavelength range or are “invisible”, i.e., strongly reduced

in intensity which is especially indicative for a symmetric ligand field around the Np(VI) central ion. After acidifications of the alkaline UV-Vis/NIR aliquots (final pH<sub>m</sub> ≈ 2), a rather broad peak with maximum at  $\lambda_{\text{max}} \approx 1262 \text{ nm}$  and  $\epsilon \approx 66 \pm 5 \text{ dm}^3 \text{ mol}^{-1} \text{ cm}^{-1}$  appeared in both cases that are obviously due to unhydrolysed Np(VI) species, see Fig. 8. The spectrum of the NpO<sub>2</sub><sup>2+</sup> aquo ion in 1 mol dm<sup>-3</sup> HCl recorded in the course of the electrochemical preparation of the initial Np(VI) stock solution, c.f. “Experimental”, is given as comparison (normalized to the same Np(VI) concentration as in the two solubility samples). Considering the great chloride concentrations ([CaCl<sub>2</sub>] = 4.5 mol dm<sup>-3</sup>), the peak at  $\lambda_{\text{max}} \approx 1262 \text{ nm}$  can reasonably be assigned to inner-sphere Np(VI) chloro complexes which would also

explain the red-shift of the peak maximum by  $\approx 42$  nm relative to the  $\text{NpO}_2^{2+}$  aquo ion. For the latter no Vis/NIR reference spectra are reported. The peak intensity of the expected Np(VI) chloro species is slightly enhanced compared to  $\text{NpO}_2^{2+}$  making a symmetric ligand environment for the former unlikely. The NEA–TDB selected data only for the first Np(VI)-chloro complex,  $\text{NpO}_2\text{Cl}^+$ , which is relevant at rather low ionic strength  $I$  and  $[\text{Cl}^-]$  (both  $\leq 4$  M) [1]. No information is available for the Np(VI)-chloro complexation behavior at greater  $I$  or  $[\text{Cl}^-]$ . Runde et al. investigated the chloro complexation of the analogous  $\text{PuO}_2^{2+}$  aquo ion in mixed LiCl + HCl media by Vis/NIR and EXAFS spectroscopy, and found evidence for the formation of  $\text{PuO}_2\text{Cl}_n^{2-n}$  inner-sphere complexes with  $n = 1-4$  [30]. In  $9 \text{ mol dm}^{-3}$  LiCl +  $1 \text{ mol dm}^{-3}$  HCl, i.e., at comparable chloride concentration as in the two Np(VI) samples analyzed by UV–Vis/NIR, the species  $\text{PuO}_2\text{Cl}_2(\text{aq})$  and  $\text{PuO}_2\text{Cl}_3^-$  are predominant. Spectral features attributed to these species are also red-shifted by ca. 13 nm and 19 nm relative to the Pu(VI) aquo ion at  $\lambda \approx 830$  nm. The overall bathochromic shift due to chloro complexation is apparently more pronounced in the case of Np(VI).

The absorption at  $\lambda_{\text{max}} \approx 984$  nm in the NIR spectrum in Fig. 8 also reveals minor contributions of Np(V) species. While the peak position in the alkaline UV–Vis/NIR sample aliquots are similar to the one of unhydrolysed Np(V) species at the same  $\text{CaCl}_2$  concentrations and  $\text{pH}_m$  values, c.f., our detailed study on the Np(V) speciation in  $\text{CaCl}_2$  solutions, the band is significantly broader (FWHM  $\approx 24.0$  nm vs.  $\approx 9$  nm), which strongly hints to the formation of complexed Np(V) species, most likely Np(V) hypochlorite complex(es) [19]. After acidification of the aliquots, which leads to the decomposition of hypochlorite and hence potential hypochlorite complexes, the Np(V) peak shows the typical band shape as reported in [19] for unhydrolyzed Np(V) in  $4.5 \text{ mol dm}^{-3}$   $\text{CaCl}_2$ . An upper limit for the Np(V) contributions of 8% of  $[\text{Np}]_{\text{tot}}$  can be estimated from the spectra. The enhanced Np solubility in  $4.5 \text{ mol dm}^{-3}$   $\text{CaCl}_2$  solutions and  $\text{pH}_m \leq 10.1$  is therefore, mainly caused by Np(VI). Note that a previous UV–Vis/NIR analysis of the same samples at  $t = 62$  days did not show any contributions of Np(V).

The UV–Vis bands of the two samples are shown in Fig. 9a. In addition to strong absorptions around  $\lambda < 350$  nm caused by the hypochlorite system, in particular  $\text{OCl}^-$  and its potential equilibrium species  $\text{Cl}_3^-$ , there are additional spectral features in the region  $\lambda \approx 300-720$  nm that can be attributed to Np(VI) species [31]. Subtraction of the spectral contributions of the hypochlorite system using the spectrum of (Np-free)  $5 \times 10^{-3} \text{ mol dm}^{-3}$  NaOCl in  $4.5 \text{ mol dm}^{-3}$   $\text{CaCl}_2$  and  $\text{pH}_m 11.0$  recorded in the present work leads to the residual

spectra shown in Fig. 9b. The spectra can be best described as a very broad and intensive multiplet showing absorptions at, e.g.,  $\lambda \approx 680$  nm with  $\varepsilon \approx 110 \pm 10 \text{ dm}^3 \text{ mol}^{-1} \text{ cm}^{-1}$ ,  $\lambda \approx 450-650$  nm with  $\varepsilon \approx 350 \pm 25 \text{ dm}^3 \text{ mol}^{-1} \text{ cm}^{-1}$  and  $\lambda \approx 390$  nm with  $\varepsilon \approx 1300 \pm 100 \text{ dm}^3 \text{ mol}^{-1} \text{ cm}^{-1}$ . Furthermore, all bands at  $\lambda < 600$  nm feature fine structures, as is, e.g., well-known for both acidic and alkaline U(VI) species, suggesting that these multiplets in the near UV and visible wavelength range are charge-transfer transitions [32]. The spectral features are different from the one of the  $\text{NpO}_2^{2+}$  aquo ion which shows less intensive absorptions at  $\lambda = 350-600$  nm with maximum extinction  $\varepsilon \approx 50 \text{ dm}^3 \text{ mol}^{-1} \text{ cm}^{-1}$ , and are likely caused by Np(VI) hydrolysis species [29]. The appearance of similar spectral features, i.e., rather intense multiplet bands in the UV–Vis region, is also reported for Np(VI)(aq) in  $2.5 \text{ mol dm}^{-3}$  NaOH solutions, where the complex  $\text{NpO}_2(\text{OH})_4^{2-}$  is expectedly predominant based on a later study of the same group [14, 33].

Despite the slightly different  $\text{pH}_m$  values (9.68 vs. 9.84) and  $[\text{Np}]_{\text{tot}}$  (factor of 2) in both samples, the deconvoluted spectra in Fig. 9b are practically identical (considering the potential uncertainties in the determination of  $[\text{Np}]$  by LSC and due to the “deconvolution” of the spectra, especially for the peak around  $\lambda = 390$  nm), indicating that the same specie(s) was predominant. Based on the discussion in the subsequent “Discussion”, and in agreement with the great overall  $[\text{Np(VI)}]$ , it is likely that oligomeric Np(VI) hydrolysis specie(s) is predominant under these conditions.

## Discussion

Contrary to the behavior of An(III), An(IV), Np(V) and U(VI) in alkaline  $\text{CaCl}_2$  solutions, and also of Np(VI) in alkaline NaCl solutions, Np(VI) solubility in alkaline  $\text{CaCl}_2$  is controlled by calcium neptunates with varying Ca-content (or solid solutions) rather than by a stoichiometric solid phase being stable over a wide range of  $\text{pH}_m$  and  $[\text{CaCl}_2]$  conditions [4, 15–17, 19–21, 27]. As a consequence, it is not (or at least not directly) possible to deduce information about the predominant Np(VI) aqueous speciation, i.e., the hydrolysis species, by simply analyzing the slope ( $\log [\text{Np(VI)}]$  vs.  $\text{pH}_m$  and vs.  $[\text{Ca}^{2+}]$ ) to get information about the potential presence of ternary Ca–Np(VI)–OH complexes of the experimental solubility curve as has been successfully done for the former cases. For the present systems, measured solubility points do not represent a ‘simple unambiguous’ entity but are related to the ( $\text{pH}_m$ ) individual solid phase compositions  $\text{Ca}_x\text{NpO}_{3+x}(\text{s,hyd})$  with  $x = 0.60-1.66$ . For a strict treatment, solid solution thermodynamics has apparently to be taken into account which relates the independent stoichiometries (and their

specific Gibbs energies of formation, or solubility constants) to a model of one or more ideal or non-ideal solid solutions (the principle equation were provided by Lippmann [34]. An excellent introduction is given in Gamsjäger et al. [35]). In the case of U(VI), Diaz Arocas et al. could successfully describe the solubility behavior of the analogous sodium polyuranates Na<sub>x</sub>UO<sub>(3+x/2)</sub>(s,hyd) (with experimental values for  $x = 0.11\text{--}0.68$  in 5 mol dm<sup>-3</sup> NaCl) by two ideal solid solutions assuming literature reported U(VI) (hydr)oxides as reasonable endmembers (UO<sub>3</sub>·2H<sub>2</sub>O/Na<sub>0.33</sub>UO<sub>3.16</sub>·2H<sub>2</sub>O and Na<sub>0.33</sub>UO<sub>3.16</sub>·2H<sub>2</sub>O/Na<sub>2</sub>U<sub>2</sub>O<sub>7</sub>) and the well-known U(VI) hydrolysis constants [25]. An analogous treatment of the Np(VI) solubility data in alkaline CaCl<sub>2</sub> solutions is currently not possible without making speculative assumptions on relevant information that is missing to properly evaluate a correct solid solution model. This is especially concerning the end member stoichiometries, their stability, as well as the Np(VI) aqueous speciation; in the process of evaluating a solid solution model, these unknowns would remain intercorrelated. For this reason, we decided that developing a solid solution model should be left out from the present study.

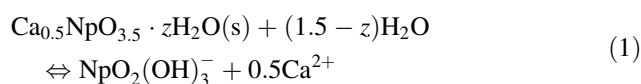
Instead, a qualitative discussion of the pH<sub>m</sub> dependence of the Np(VI) solubility data in alkaline CaCl<sub>2</sub> solutions is provided in the following. It is based on the assumption that the differences in the solid phase stability (the solubility products) of Ca<sub>x</sub>NpO<sub>3+x</sub>(s,hyd) in a narrow pH<sub>m</sub> range (and hence, for similar values of  $x$ , c.f. Fig. 3) is not too big, and consequently, that a qualitative slope analysis (log [Np(VI)] vs. pH<sub>m</sub>) is still possible without following the stricter solid solution approach. This assumption is not too digressive. If there was a very strong change in the solid phase stability for the independent calcium neptunate compositions, one of the compositions should actually be stable over a wider range of pH<sub>m</sub> values. This is apparently not the case as the Ca-content in the calcium neptunates and the pH<sub>m</sub> values in the solubility samples are continuously correlated, see Fig. 3.

Based on the hydrolysis schemes valid for Np(VI) and U(VI) in alkaline NaCl and at relatively low total [An(VI)], as it is the case for solubility controlled equilibrium reactions, the third and fourth hydrolysis complex of Np(VI), NpO<sub>2</sub>(OH)<sub>3</sub><sup>-</sup> and NpO<sub>2</sub>(OH)<sub>4</sub><sup>2-</sup>, have to be considered as most relevant Np(VI) species in the systems [1, 4]. Although the limiting complex NpO<sub>2</sub>(OH)<sub>5</sub><sup>3-</sup> (representing the case that all five water ligands of the NpO<sub>2</sub><sup>2+</sup> aquo are replaced by OH<sup>-</sup>) only starts to form at very high alkalinity ([OH<sup>-</sup>] ≥ 3.5 mol dm<sup>-3</sup>) in non or weakly complexing Li<sup>+</sup>, Na<sup>+</sup> and TMA<sup>+</sup> solutions [14], it is still considered in the discussion, as Ca<sup>2+</sup> can significantly enhance the hydrolysis by the formation of Ca-specific ternary Ca–M–OH complexes, as already discussed. Furthermore, and based on the information available for the analogous U(VI)

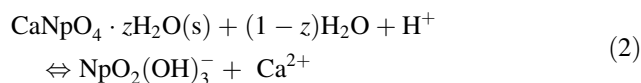
and Pu(VI) systems, formation of oligomeric Np(VI) species might be relevant for certain Np(VI) solubility samples, especially the ones showing the greatest solubility.

### Samples with [CaCl<sub>2</sub>] = 0.25–2.0 mol dm<sup>-3</sup> and pH<sub>m</sub> < 10.1

In alkaline NaCl solutions with pH<sub>m</sub> < 11, NpO<sub>2</sub>(OH)<sub>3</sub><sup>-</sup> is the predominant Np(VI) species for low [Np(VI)]<sub>tot</sub> (absence of oligomeric species). If this species was in equilibrium with stoichiometric solid phases of the composition Ca<sub>0.5</sub>NpO<sub>3.5</sub>(s,hyd) and CaNpO<sub>4</sub>(s,hyd), respectively, what approximately reflects the range of calcium contents in Ca<sub>x</sub>NpO<sub>3+x</sub>(s,hyd) for 8.5 < pH<sub>m</sub> < 10.5, the corresponding solubility curves would reveal slopes (log [Np(VI)] vs. pH<sub>m</sub>) of 0 and - 1:

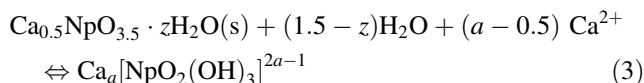


and

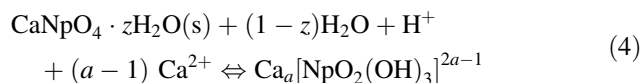


The experimental values for the samples with [CaCl<sub>2</sub>] = 0.25–2.0 mol dm<sup>-3</sup> and pH<sub>m</sub> < 10.1 displayed in Fig. 6f are indeed around - 0.25 and - 0.65, and are therefore in good qualitative agreement with the extreme cases for stoichiometric solids represented by Eqs. (1) and (2).

The solubility in these samples also shows a systematic increase with [CaCl<sub>2</sub>]. If binary NpO<sub>2</sub>(OH)<sub>3</sub><sup>-</sup> was actually the predominant species, the opposite is qualitatively expected: according to Eqs. (1) and (2), greater [CaCl<sub>2</sub>] in solution shifts the equilibrium to the left hand side, i.e., stabilizes the calcium containing solid phase and decreases log [Np(VI)]. Both, the pH<sub>m</sub> dependence and the strong dependence on [CaCl<sub>2</sub>] could be explained if the third Np(VI) hydrolysis complex in alkaline CaCl<sub>2</sub> solutions existed as ternary species Ca<sub>a</sub>[NpO<sub>2</sub>(OH)<sub>3</sub>]<sup>2a-1</sup> (with  $a > 0$ ),



and

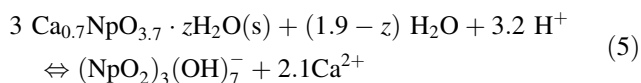


Contrary to Eqs. (1) and (2), the number of Ca<sup>2+</sup> being consumed exceeds or is equal to the one being released in the equilibrium reaction, which favors a positive dependence of the complex formation at greater [CaCl<sub>2</sub>]. While this

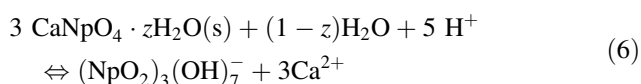
qualitative assessment neglects the changing activity in the different  $\text{CaCl}_2$  solutions, more quantitative scoping calculations taking into account the present SIT (specific ion interaction theory) activity model for Np(VI) and  $\text{CaCl}_2$  lead to the same conclusion (calculations not shown) [1, 4].

### Samples with $[\text{CaCl}_2] = 3.5\text{--}4.5 \text{ mol dm}^{-3}$ and $\text{pH}_m \approx 10.0$

The solubility of the samples with  $[\text{CaCl}_2] = 3.5\text{--}4.5 \text{ mol dm}^{-3}$  and  $\text{pH}_m \approx 10$  depends more pronounced on  $\text{pH}_m$  (slopes of  $\approx -4$ ) compared to the systems with lower  $[\text{CaCl}_2]$ , see Fig. 6f. This can hardly be explained by equilibrium reactions with the monomeric hydrolysis species  $\text{NpO}_2(\text{OH})_n^{2-n}$  with  $n = 3\text{--}5$  considered here. As discussed in the previous sections, the enhanced  $[\text{Np}]_{\text{tot}}$  is also not due to Np(VI) hypochlorito complexes, or Np(V). Although so far not reported, the existence of oligomeric, anionic hydrolysis species of Np(VI) at greater  $[\text{Np(VI)}]_{\text{tot}}$  is not unlikely (provided that greater  $[\text{Np(VI)}]_{\text{tot}}$  are stable towards precipitation), as the principle existence of Np(VI) oligomers was demonstrated in acidic condition ( $(\text{NpO}_2)_3(\text{OH})_5^+$ ), and as such species exist for the analogous and well-studied U(VI) system (also in the case of Pu(VI), oligomeric hydrolysis species become relevant at  $[\text{Pu(VI)}]_{\text{tot}} \geq 1 \times 10^{-4} \text{ mol dm}^{-3}$  in near-neutral solutions as described in [36]). Based on the data selected for U(VI) in the NEA-TDB,  $\text{UO}_2(\text{OH})_3^-$  (at lower  $[\text{U}]_{\text{tot}}$ ) and the trimeric anionic complex,  $(\text{UO}_2)_3(\text{OH})_7^-$  (at greater  $[\text{U}]_{\text{tot}}$ ) are the predominant U(VI) species under similar  $\text{pH}_m$  conditions [1]. Further oligomeric species like  $(\text{UO}_2)_3(\text{OH})_8^{2-}$  were postulated [the corresponding experiments were performed in weakly complexing TMAOH solutions to avoid precipitation of U(VI)-(hydr)oxide solid phases] [32]. Orienting predominance diagrams for Np(VI) and U(VI) aqueous speciation calculated for  $I = 0$  are shown in Fig. 10. Assuming that the analogous species  $(\text{NpO}_2)_3(\text{OH})_7^-$  existed, the slopes of the solubility curves in equilibrium with stoichiometric solid phases with Ca:Np ratios in the range 0.7:1–1:1 would be in the range  $\approx -3$  to  $-5$ , i.e., rather steep:



and

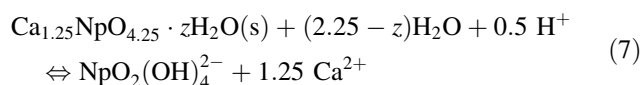


Formulation with a hypothetical  $(\text{NpO}_2)_3(\text{OH})_8^{2-}$  complex leads to similar values. The experimental slopes in Fig. 6f are around  $-4$ , so that Eqs. (5) and (6) could

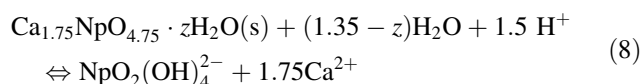
reasonably explain the enhanced solubility at  $[\text{CaCl}_2] = 3.5$  and  $4.5 \text{ mol dm}^{-3}$  at  $\text{pH}_m \approx 10$ . More systematic studies on that topic are required to confirm the relevance of oligomeric Np(VI) hydrolysis species.

### Samples with $[\text{CaCl}_2] = 0.25\text{--}4.5 \text{ mol dm}^{-3}$ and $\text{pH}_m > 11.0$

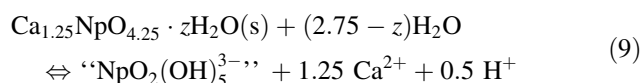
For more alkaline solutions with  $\text{pH}_m > 11.0$ ,  $\text{NpO}_2(\text{OH})_4^{2-}$  and the rather hypothetical  $\text{NpO}_2(\text{OH})_5^{3-}$  are considered as predominant species. In equilibrium with the stoichiometric compounds  $\text{Ca}_{1.25}\text{NpO}_{4.25} \cdot z\text{H}_2\text{O}(\text{s})$  and  $\text{Ca}_{1.75}\text{NpO}_{4.75} \cdot z\text{H}_2\text{O}(\text{s})$ , which covers the compositions of the solubility controlling calcium neptunates in this  $\text{pH}_m$  range, the corresponding slopes ( $\log [\text{Np}]$  vs.  $\text{pH}_m$ ) would be  $-0.5$  and  $-1.5$ , as well as  $-0.5$  and  $+0.5$ , respectively:



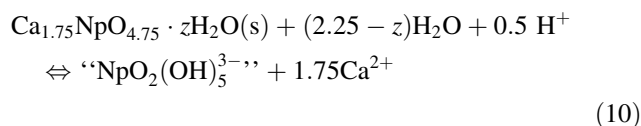
and



and



and



The experimental solubility curves for  $\text{pH}_m > 11.0$  do not show a strong dependence on  $\text{pH}_m$ , i.e., are around 0. The ‘slope profiles’ for the (1, 5) complex fit better to the experimental data (combination of a positive slope at lower  $\text{pH}_m$  and a negative slope at greater  $\text{pH}_m$ ). A potential (1, 5) complex could, however, hardly exist as binary species with charge  $-3$  in presence of  $\text{Ca}^{2+}$ , but would be stabilized/complexed as ternary species  $\text{Ca}_b[\text{Np}(\text{OH})_5]^{2b-3}$ . The presence of calcium containing Np(VI) hydrolysis complexes in this  $\text{pH}_m$  range is actually required to explain the rather insignificant dependence on  $[\text{CaCl}_2]$  observed as any calcium in the hydrolysis species partly compensates (or even supercompensates) for the number of calcium ions released from the dissolution of the solid phases according to Eqs. (7) to (10), see analogous discussion for the samples with  $[\text{CaCl}_2] = 0.25\text{--}2.0 \text{ mol dm}^{-3}$  and  $\text{pH}_m < 10.1$ .

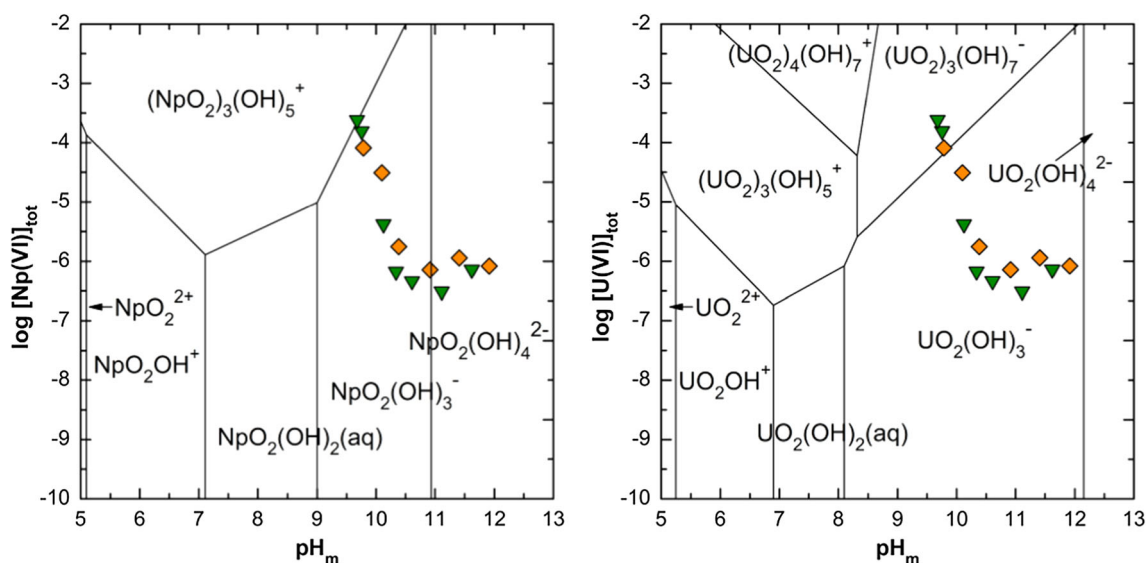


**Fig. 10** Orienting predominance diagram of aqueous Np(VI) and U(VI) speciation at  $I = 0$  calculated with data from NEA–TDB and Gaona et al. (for Np) [1, 4]. For a qualitative comparison, the

solubility data of Np(VI) in  $3.5 \text{ mol dm}^{-3}$  (diamonds) and  $4.5 \text{ mol dm}^{-3}$  (triangles) CaCl<sub>2</sub> solutions are displayed for both diagrams

## Conclusions

The present work represents the first systematic investigation of the Np(VI) solubility in alkaline  $0.25\text{--}4.5 \text{ mol dm}^{-3}$  CaCl<sub>2</sub> solutions. As solubility limiting Np(VI) solid phases, so far not reported non-stoichiometric calcium neptunates, Ca<sub>*x*</sub>NpO<sub>3+*x*</sub>(s,hyd), were identified with a calcium content systematically ranging from  $x = 0.60$  to  $1.66$ . The different solid phase compositions formed in the independent batch solubility samples from the same initial Ca<sub>1.28</sub>NpO<sub>4.28</sub>(s,hyd), and were systematically correlated to the individual pH<sub>m</sub> values in the solutions (but not to different [CaCl<sub>2</sub>]). The corresponding XRD patterns are similar, but not identical, and hint to related crystal structures where the calcium can apparently quickly exchange.

In most of the samples, stable Np(VI) solubility data were observed from  $t \approx 60$  days to the last sampling after  $t \approx 430$  days. For all systems with [CaCl<sub>2</sub>] =  $0.25\text{--}2.0 \text{ mol dm}^{-3}$  as well as for the ones with [CaCl<sub>2</sub>] >  $2.0 \text{ mol dm}^{-3}$  and pH<sub>m</sub> >  $10.5$ , the experimental solubility curves are in agreement with monomeric NpO<sub>2</sub>(OH)<sub>*n*</sub><sup>2-*n*</sup> with  $n = 3\text{--}5$  as the predominant aqueous Np(VI) species. The systematic dependence of [Np(VI)] on [CaCl<sub>2</sub>] further indicates a strong and specific ion interaction between the anionic NpO<sub>2</sub>(OH)<sub>*n*</sub><sup>2-*n*</sup> and Ca<sup>2+</sup>, or even the formation ternary complexes of the type Ca<sub>*a*</sub>[NpO<sub>2</sub>(OH)<sub>*n*</sub>]<sup>2*a*+2-*n*</sup>, as recently described for anionic hydrolysis species of An(III)–An(V) in alkaline CaCl<sub>2</sub> solutions. The strongly pH<sub>m</sub> dependent (slope  $\approx -4$ ), enhanced solubility observed for systems with [CaCl<sub>2</sub>] =  $3.5\text{--}4.5 \text{ mol dm}^{-3}$

and pH<sub>m</sub>  $9.5\text{--}10.0$  is likely due to an equilibrium between Ca<sub>*x*</sub>NpO<sub>3+*x*</sub>(s,hyd) and so far not reported anionic, oligomeric Np(VI)-hydrolysis complexes (these species are well-known under comparable conditions for the analogous U(VI) systems) for which UV–Vis/NIR data are provided.

The present work reveal significant differences in the solid phase formation of Np(VI) in alkaline CaCl<sub>2</sub> solutions compared to the analogous U(VI) system, where the solubility under neutral to hyperalkaline pH<sub>m</sub> conditions is controlled by the stoichiometric phase CaU<sub>2</sub>O<sub>7</sub>·3H<sub>2</sub>O(cr), and by metaschoepite UO<sub>3</sub>·2H<sub>2</sub>O(cr) in acidic solutions. Although substoichiometric becquerelite CaU<sub>6</sub>O<sub>9</sub>·11H<sub>2</sub>O(cr) is well-known, and can control the U(VI) solubility in a narrow pH<sub>m</sub> region limited by the thermodynamic stability fields of the two former phases, no evidence for a solubility controlling calcium polyuranate with continuously changing calcium content exists for U(VI) in CaCl<sub>2</sub> solutions. On the other hand, the behavior of Np(VI) in CaCl<sub>2</sub> solutions shows some similarities to U(VI) in near-neutral NaCl solutions, where the relevance of sodium polyuranates Na<sub>*x*</sub>UO<sub>(3+*x*/2)</sub>(s,hyd) (with  $x$  going from  $0.11$  to  $0.68$  in  $5.0 \text{ mol dm}^{-3}$  NaCl) as solubility controlling U(VI) solid phases, i.e., in between the thermodynamic stability of the stoichiometric metaschoepite and Na<sub>2</sub>U<sub>2</sub>O<sub>7</sub>·H<sub>2</sub>O(cr), was demonstrated.

The results of the present study with Np(VI) and the reported literature case of U(VI) confirm the relevance of poly(hydr)oxides solid phases of hexavalent actinides (or solid solutions) under certain solution conditions for an improved understanding and quantitative thermodynamic description of actinide solubility and speciation.

## Experimental

All experiments were performed under argon (Ar) atmosphere in an glove box at room temperature ( $t = 23 \pm 2$  °C). Ultrapure water (Milli-Q academic, Millipore; purged with Ar before use) and  $\text{CaCl}_2 \cdot 2\text{H}_2\text{O}$  (p.a., Merck) were used to prepare pH neutral stock solutions with  $[\text{CaCl}_2] = 0.25, 1.0, 2.0, 3.5,$  and  $4.5 \text{ mol dm}^{-3}$  (0.252, 1.02, 2.11, 3.91, and 5.26 mol (kg  $\text{H}_2\text{O}$ ) $^{-1}$ , c.f. [16, 19]. Aliquots of the latter were equilibrated with  $\text{Ca}(\text{OH})_2$  (s) [freshly prepared under argon atmosphere by addition of one equivalent of a 4.0 mol  $\text{dm}^{-3}$  NaOH solution with low carbonate content to an acidic 2.0 mol  $\text{dm}^{-3}$   $\text{CaCl}_2$  solution with  $\text{pH}_m \approx 3$ , and washing the precipitate several times with water] to obtain the corresponding alkaline  $\text{CaCl}_2$  solutions at maximum  $\text{pH}_m$  11.7–12.1, c.f. [16, 19]. Appropriate aliquots of the pH neutral and alkaline (after removing the calcium hydroxide or hydroxychloride precipitate by centrifugation)  $\text{CaCl}_2$  stock solutions of the same ionic strength were mixed to obtain series of matrix solutions with  $\text{pH}_m$  8.5–12 for the batch solubility samples. To minimize carbonate impurities found in the commercial product, NaOCl was in-house prepared by introducing chlorine gas [in situ produced by reaction of concentrated HCl solution (suprapur, Merck) with solid  $\text{KMnO}_4$  (p.a., Merck)] into 2 mol  $\text{dm}^{-3}$  NaOH solution (dilute it, Baker) under argon atmosphere at 0 °C applying classical Schlenk technique. The final solution contained  $[\text{NaOCl}] = 0.71 \pm 0.04 \text{ mol dm}^{-3}$ ,  $[\text{NaOH}] = \sim 0.6 \text{ mol dm}^{-3}$ , as determined by redox titration and pH measurement, and consequently  $[\text{NaCl}] \sim 0.7 \text{ mol dm}^{-3}$ . The total inorganic carbon concentration was determined as  $3 \times 10^{-3} \text{ mol dm}^{-3}$  by a commercial  $\text{CO}_2$  analyzer (TOC 5000, Schimadzu). This is irrelevant in view of the very minor amounts of NaOCl solution added to the samples to fix strongly oxidizing conditions. As primary Np source, an ion exchange column purified and isotopically pure 0.32 mol  $\text{dm}^{-3}$   $^{237}\text{Np}(\text{V})$  stock solution in dilute HCl was used. The latter was thoroughly characterized by liquid scintillation counting (LSC), inductively coupled plasma mass spectrometry (ICP-MS) and gamma spectrometry. The oxidation state of Np(V) was confirmed by Vis/NIR absorption spectroscopy (Cary 5e, Varian). No alpha emitters other than  $^{237}\text{Np}$  were detected by alpha spectrometry.

### Measurements of pH, $E_h$ , [Np] and Vis/NIR absorption spectroscopy

The molal proton concentration  $m(\text{H}^+)$  ( $\text{pH}_m = -\log\{m(\text{H}^+)/\text{mol (kg H}_2\text{O)}^{-1}\}$ ) in the samples was determined with glass/ROSS combination electrodes (Orion, 3 mol  $\text{dm}^{-3}$  KCl as filling solution) calibrated

before and after each sampling against dilute standard pH buffer solutions (pH 6–13, Merck). Measured values  $\text{pH}_{\text{exp}}$  were converted to  $\text{pH}_m$  according to the relation  $\text{pH}_m = \text{pH}_{\text{exp}} + A_m$ , with  $A_m = -0.01, 0.33, 0.83, 1.71,$  and 2.41 for  $[\text{CaCl}_2] = 0.252, 1.02, 2.11, 3.91,$  and 5.26 mol (kg  $\text{H}_2\text{O}$ ) $^{-1}$  [16].

Experimental redox potentials in the samples were measured with a combined Pt/Ag–AgCl ring electrode (Metrohm, 3 mol  $\text{dm}^{-3}$  KCl as salt bridge) in the clear supernatant solution under careful stirring and without suspending of the Np(VI) solid phase. Stable readings were typically obtained after 5–15 min, and converted into  $E_h$  (and pe values with  $\text{pe} = 16.9 \times E_h$  at  $T = 25$  °C) by correcting for the measured potential of the Ag–AgCl reference electrode,  $E_h = E_{\text{read}} \text{ (mV)} + 208 \text{ mV}$ . As no further correction for the liquid junction potentials were applied,  $E_h$  (pe) values only represent qualitative indications of the redox milieu in the samples, especially for the highly concentrated  $\text{CaCl}_2$  systems. The proper functioning of the electrode was tested with a standard redox buffer solution (+ 640 mV vs. Ag–AgCl, Schott) at regular intervals.

[Np] was routinely measured after ultrafiltration (10 kD  $\approx 2$  nm, Pall Life Science) by liquid scintillation counting of the alpha activity after discrimination of the beta counts from the daughter  $^{233}\text{Pa}$  on a Quantulus low level counter (Wallace) using Ultima Gold XR cocktail (Perkin-Elmer). The detection limit is approximately  $1 \times 10^{-9} \text{ mol dm}^{-3}$  for  $^{237}\text{Np}$ .

For ultraviolet–visible/near-infrared (UV–Vis/NIR) absorption investigations, aliquots of the supernatant solutions of selected solubility samples (alkaline  $\text{pH}_m$ ) were filled into air-tight screw cap quartz cuvettes (Hellma QS, pathlength 1 cm) inside the argon box and measured outside of the box on a Cary 5e (Varian) in the range 1350–250 nm (double beam mode, data interval 0.2 nm, scan rate 60 nm/min, spectral bandwidth SBW 0.7 nm). A second spectrum was acquired directly after addition of a few microliters of 4.0 mol  $\text{dm}^{-3}$  HCl to the UV–Vis/NIR sample aliquot to obtain a final  $\text{pH}_m \approx 2$ .

### Preparation and characterization of the solubility limiting Np(VI) solid phase

Approximately 215 mg of Np(V), i.e., 2.8  $\text{cm}^3$  of the Np(V) stock solution, were diluted in 9.2  $\text{cm}^3$  of 1 mol  $\text{dm}^{-3}$  HCl and quantitatively oxidized to Np(VI) in an electrochemical cell at  $E_{\text{anode}} = +1.3 \text{ V}$  (Pt grid working electrode, Pt counter electrode from Metrohm, Ag–AgCl reference electrode from Metrohm, potentiostat from Princeton Applied Research). The reaction progress was regularly monitored by Vis/NIR absorption spectroscopy. The spectrum of the final solution showed only

the features reported for Np(VI) in 2 mol dm<sup>-3</sup> HClO<sub>4</sub> while all peaks of the initial Np(V) were absent, see Fig. 8 [29].

Aliquots of 100 mm<sup>3</sup> of the Np(VI) solution were added stepwise to 190 cm<sup>3</sup> of a 4.5 mol dm<sup>-3</sup> CaCl<sub>2</sub>/5 × 10<sup>-3</sup> mol dm<sup>-3</sup> NaOCl solution with pH<sub>m</sub> ≈ 11.4 and (measured) E<sub>h</sub> = 0.82 V which resulted in the precipitation of a brown, fluffy solid phase. The pH<sub>m</sub> value was monitored during addition of the acidic Np(VI) solution and kept in the range of pH<sub>m</sub> 10.6–11.4 by spiking small aliquots of a Ca(OH)<sub>2</sub> suspension. The final composition of the sample was [CaCl<sub>2</sub>] = 4.2 mol dm<sup>-3</sup>, [NaOCl] = 4.5 × 10<sup>-3</sup> mol dm<sup>-3</sup>, pH<sub>m</sub> 11.2, E<sub>h</sub> ≈ 0.9 V. Following 2 months of equilibration under the mother solution the precipitate was characterized and used as starting material for the batch solubility experiments; see “Results and discussion”. At the end of the study, equilibrium solid phases from selected batch samples were re-analyzed.

For the characterizations, 1–3 mg of the Np(VI) equilibrium solid phase of a batch sample were separated from the solution and washed 3–6 times with 1 cm<sup>3</sup> of ethanol. Adequate amounts of the dried solids were then analyzed by powder X-ray diffraction (D8 Advance, Bruker), and in one case, by combined scanning electron microscopy + energy dispersive X-ray spectrometry (SEM–EDX, CamScan CS 44 FE, Cambridge Instruments). For the quantitative determination of structural calcium and neptunium contents in the solid phases, the dried materials were dissolved in 2% HNO<sub>3</sub> and independently analyzed by inductively coupled plasma–optical emission spectroscopy (ICP–OES, Optima 2000, Perkin-Elmer) and LSC, respectively.

### Solubility experiments

For the undersaturation batch solubility experiments, fractions of 5–15 mg of the characterized Np(VI) starting solid phase were equilibrated in 30 cm<sup>3</sup> of 0.25, 1.0, 2.0, 3.5, and 4.5 mol dm<sup>-3</sup> CaCl<sub>2</sub> solutions at pH<sub>m</sub> 8.5–12.0 (6–7 independent samples per CaCl<sub>2</sub> series) in 42 cm<sup>3</sup> centrifuge tubes (polypropylene, Nalgene). All samples of this “main series” contained 5 × 10<sup>-3</sup> mol dm<sup>-3</sup> NaOCl as oxidizing agent to stabilize hexavalent neptunium. To test possible specific interactions between Np(VI) and NaOCl, especially complexation reactions, an additional series of seven samples with [CaCl<sub>2</sub>] = 0.25 and 2.0 mol dm<sup>-3</sup>, pH<sub>m</sub> 9.0–11.5, and [NaOCl] = 5 × 10<sup>-2</sup> mol dm<sup>-3</sup> and 5 × 10<sup>-4</sup> mol dm<sup>-3</sup> was studied, for which approximately one half of the Np(VI) equilibrium solid phases from the samples of the main series with the same [CaCl<sub>2</sub>] and closest pH<sub>m</sub> values were used after 100 days (after adequate washing steps with the corresponding new matrix solutions). All samples were analyzed for [Np],

pH<sub>m</sub>, and E<sub>h</sub> as function of time for *t* = 430 days (main series) and *t* = 330 days (additional series), respectively. In most cases, seven independent samplings were performed (3 in the case of the additional series). The results of the samplings are provided as electronic supplementary material.

### X-ray absorption fine structure (XAFS) spectroscopy

Np(VI) equilibrium solid phases retrieved after *t* = 140 days from two representative batch samples in 2 mol dm<sup>-3</sup> CaCl<sub>2</sub> at pH<sub>m</sub> 9.3 and 11.8, respectively, were additionally studied by Np L<sub>3</sub>-edge XAFS (X-ray Absorption Fine Structure) at the 2.5 GeV synchrotron light source ANKA, KIT Campus North, at the INE-Beamline for actinide research [37]. About 3 mg of the solids were centrifuged to form a stable precipitate at the tip of sealed 200 mm<sup>3</sup> vials (polypropylene, Eppendorf) and in situ measured as wet pastes, i.e., without removing the remaining matrix solution. Sample vials were mounted inside an Ar-flushed cell which acts as second containment, at the same time keeping sample vials inside an inert gas atmosphere during transport and data acquisition.

In the present work, only the information obtained from the XANES (X-ray Absorption Near Edge Structure) spectra are discussed while results from the EXAFS (extended XAFS) evaluation, i.e., structural parameters, will be subject of a subsequent publication. The XAFS measurements of the Np(VI) solid phases were performed within the same campaign as the Np(V) samples of our related solubility study [19]. Details of the XAFS data collection and treatment are reported there. All Np L<sub>3</sub>-XAFS spectra were recorded in fluorescence detection mode by registering the Np L<sub>α</sub> fluorescence yield at ~ 13.95 keV as function of the incident photon energy with a 5-pixel Ge solid state detector (Canberra LEGe). Up to 6 scans were collected at room temperature and averaged for each sample. XANES spectra were isolated from XAFS scans following subtraction of a linear pre-edge background function and normalization of the edge jump to unity.

**Acknowledgements** Technical support by V. Petrov (Moscow State University), S. Moisei-Rabung and P. Leske (KIT—Institute for Nuclear Waste Disposal) is gratefully acknowledged.

### References

1. Guillaumont R, Fanghänel Th, Fuger J, Grenthe I, Neck V, Palmer DA, Rand MH (2003) Chemical thermodynamics vol. 5, update on the chemical thermodynamics of uranium, neptunium, plutonium, americium and technetium. Elsevier, North-Holland

2. Morss LR, Edelstein NM, Fuger J (2008) The chemistry of the actinide and transactinide elements. Springer, Dordrecht
3. Neck V, Altmaier M, Fanghänel T (2007) *C R Chim (France)* 10:959
4. Gaona X, Fellhauer D, Altmaier M (2013) *Pure Appl Chem* 85:2027
5. Cassol A, Magon L, Tomat G, Portanova R (1972) *Inorg Chem* 11:515
6. Kato Y, Kimura T, Yoshida Z, Nitani N (1996) *Radiochim Acta* 74:21
7. Gaona X, Tits J, Dardenne K, Liu X, Denecke MA, Wieland E, Altmaier M (2012) *Radiochim Acta* 100:759
8. Bagnall KW, Laidler JB (1964) *J Chem Soc* 2693. <https://doi.org/10.1039/jr9640002693>
9. Saito T, Wang J, Kitazawa T, Takahashi M, Takeda M, Nakada M, Nakamoto T, Masaki NM, Yamashita T, Saeki M (1999) *Radioanal Nucl Chem* 239:319
10. Keller C, Koch L, Walter KH (1965) *J Inorg Nucl Chem* 27:1205
11. Williams CW, Blaudeau J-P, Sullivan JC, Antonio MR, Bursten B, Soderholm L (2001) *J Am Chem Soc* 123:4346
12. Bolvin H, Wahlgren U, Moll H, Reich T, Geipel G, Fanghänel T, Grenthe I (2001) *J Phys Chem A* 105:11441
13. Gaona X, Wieland E, Tits J, Scheinost A, Dähn R (2013) *Appl Geochem* 28:109
14. Clark DL, Conradson SD, Donohoe RJ, Gordon PL, Keogh DW, Palmer PD, Scott BL, Tait CD (2013) *Inorg Chem* 52:3547
15. Neck V, Altmaier M, Rabung T, Lützenkirchen J, Fanghänel T (2009) *Pure Appl Chem* 81:1555
16. Altmaier M, Neck V, Fanghänel T (2008) *Radiochim Acta* 96:541
17. Fellhauer D, Neck V, Altmaier M, Lützenkirchen J, Fanghänel T (2010) *Radiochim Acta* 98:541
18. Yalcintas E, Gaona X, Altmaier M, Dardenne K, Polly R, Geckeis H (2016) *Dalton Trans* 45:8916
19. Fellhauer D, Rothe J, Altmaier M, Neck V, Runke J, Wiss T, Fanghänel T (2016) *Radiochim Acta* 104:355
20. Fellhauer D, Altmaier M, Gaona X, Lützenkirchen J, Fanghänel T (2016) *Radiochim Acta* 104:381
21. Altmaier M, Neck V, Müller R, Fanghänel T (2005) Abstract No. A1-3, 10th international conference on chemistry and migration behaviour of actinides and fission products in the geosphere. Avignon, France
22. Vochten R, van Haverbeke L (1990) *Mineral Petrol* 43:65
23. Sandino MCA, Grambow B (1994) *Radiochim Acta* 66/67:37
24. Rai D, Felmy AR, Hess NJ, LeGore VL, McCready DE (2002) *Radiochim Acta* 90:495
25. Diaz Arocas P, Grambow B (1998) *Geochim Cosmochim Acta* 62:245
26. Allen PG, Shuh DK, Bucher JJ, Edelstein NM, Palmer CEA, Silva RJ, Nguyen SN, Marquez LN, Hudson EA (1996) *Radiochim Acta* 75:47
27. Altmaier M, Yalcintas E, Gaona X, Neck V, Müller R, Schlieker M, Fanghänel T (2017) *J Chem Therm* 114:2
28. Pashalidis I, Kim JJ, Lierse C, Sullivan JC (1993) *Radiochim Acta* 60:99
29. Hagan PG, Cleveland JM (1966) *J Inorg Nucl Chem* 28:2905
30. Runde W, Neu MP, Conradson SD, Clark DL, Palmer PD, Reilly SD, Scott BL, Tait CD (1996) *Mat Res Soc Symp Proc* 465:693
31. Hartmann T, Paviet-Hartmann P, Wetteland C, Lu N (2003) *Rad Phys Chem* 66:335
32. Nguyen-Trung C (2002) Ph.D. thesis, University of Nancy
33. Clark DL, Conradson SD, Neu MP, Palmer PD, Runde W, Tait CD (1997) *J Am Chem Soc* 119:5259
34. Lippmann F (1977) *Neues Jahrb Mineral. Abh* 130:243
35. Gamsjäger H, Königsberger E, Preis W (2000) *Aquat Geochem* 6:119
36. Reilly SD, Neu MP (2006) *Inorg Chem* 45:1839
37. Rothe J, Butorin S, Dardenne K, Denecke MA, Kienzler B, Löble M, Metz V, Seibert A, Steppert M, Vitova T, Walther C, Geckeis H (2012) *Rev Sci Instrum* 83:1